

# Ring diagram analysis of the characteristics of solar oscillation modes in active regions

S. P. Rajaguru

*Indian Institute of Astrophysics, Bangalore-560 034, India*

rajguru@iiap.ernet.in

Sarbani Basu

*Astronomy Department, Yale University, P. O. Box 208101, New Haven CT 06520-8101, U.S.A.*

basu@astro.yale.edu

and

H. M. Antia

*Tata Institute of Fundamental Research, Homi Bhabha Road, Mumbai 400005, India*

antia@tifr.res.in

## ABSTRACT

The presence of intense magnetic fields in and around sunspots is expected to modify the solar structure and oscillation frequencies. Applying the ring diagram technique to data from the Michelson Doppler Imager (MDI) on board the Solar and Heliospheric Observatory (SOHO), we analyze the characteristics of high-degree f and p modes near active regions and compare them with the characteristics of the modes in quiet regions. As expected from earlier results, the f- and p-mode frequencies of high degree modes are found to be significantly larger in magnetically active regions. In addition, we find that the power in both f and p modes is lower in active regions, while the widths of the peaks are larger, indicating smaller lifetimes. We also find that the oscillation modes are more asymmetric in active regions than those in quiet regions, indicating that modes in active regions are excited closer to the surface. While the increase in mode frequency is monotonic in frequency, all other characteristics show more complex frequency dependences.

*Subject headings:* Sun: oscillations; Sun: activity

## 1. Introduction

The solar activity cycle is marked by the appearance of sunspots, which are regions of intense magnetic field. The presence of these magnetic fields in and around sunspots in and below the photosphere modifies the equilibrium profile of sound speed and density, through the Lorentz force. This change in the properties of localized regions in the Sun is expected to modify the characteristics of solar f and p modes. Sunspots are known to scatter and absorb p modes, as found by the early observations (Braun, LaBonte & Duvall 1987, 1988, 1990; Braun 1995). Despite a number of subsequent studies in this field (see e.g., Hollweg (1988); Rosenthal (1990); Bogdan et al. (1993); Keppens, Bogdan & Goossens (1994); Bogdan et al. (1996)), the exact mechanism of the phenomenon remains unknown. It is also well known that amplitudes of solar oscillations decrease significantly in active regions (Tarbell et al. 1988; Hindman & Brown 1998). It is not clear if the decrease in power is due to absorption of acoustic modes by sunspots or due to weaker excitation in active regions. High degree modes, i.e., those with very short horizontal wavelengths, are expected to be affected the most by sunspots. The lifetime of these modes is much smaller than the sound travel time around the Sun, and therefore, local effects are more important for these modes than for low-degree modes which have much larger horizontal wavelengths and also longer life-times.

With the availability of data from the Michelson Doppler Imager (MDI) on board the SOHO spacecraft, it is now possible to look at small areas around a sunspot. In this work, we make a detailed comparative study of the properties of high-degree oscillation modes in active and quiet regions. We study how the different mode-characteristics vary with the mean magnetic field of the active regions. We use the ring diagram technique (Hill 1988) for our analysis.

The temporal variation of the mean frequencies, as well as other characteristics of global modes of oscillations with solar cycle, has been extensively studied (Elsworth et al. 1990; Libbrecht & Woodard 1990; Dziembowski et al. 1998; Bhatnagar, Jain & Tripathy 1999; Howe, Komm & Hill 1999). This variation is likely to be due to the variation in the global magnetic field over the solar cycle. The magnetic field in sunspot regions is much stronger than the average field during maximum activity, and hence, we expect a much larger effect if modes in active regions are studied separately. This will also compensate for the larger statistical errors of the ring diagram analysis technique as compared with global mode analysis techniques, mainly due to smaller spatial and temporal intervals covered by the ring diagram analysis.

Temporal variations in large scale flows using ring diagram analysis have been studied extensively (Patrón et al. 1998; Basu & Antia 1999, 2000). Haber et al. (2001) have studied both the temporal and spatial variation in flow velocities. This includes the variation in flow

velocity with the magnetic field of active regions. Although no clear systematic variation in flows with magnetic field in active regions is found, Haber et al. (2001) claim that horizontal flows are faster in active regions as compared to quiet regions, and that flows converge around active regions. Hindman et al. (2001) have tried to study variation in mode frequencies with magnetic field. They find that mean frequencies of oscillations increase with magnetic field in the region being considered. Furthermore, the frequency shifts relative to the temporal and spatial average are found to trace the active regions.

In this work, apart from frequencies and power variation we also include other important characteristics of modes viz., width and asymmetry of peak profiles. We also study variation in background power between pairs of active and quiet regions. The rest of the paper is organized as follows: we briefly discuss the analysis technique and describe the data used in Section 2, present the results in Section 3, and discuss the results and summarize our conclusions in Section 4.

## 2. The Analysis

Ring diagrams are three-dimensional (3D) power spectra of short-wavelength modes in a small region of the Sun. High-degree (short wavelength) modes can be approximated as plane waves over a small area of the Sun as long as the horizontal wavelength of the modes is much smaller than the area covered. Ring diagrams are obtained from a time series of Dopplergrams of a specific area of the Sun tracked with the mean rotation velocity. The 3D Fourier transform of this time series gives the power spectra. These power spectra are often referred to as ring diagrams because of the characteristic ring-like shape of the power in sections of constant temporal frequency. A detailed description of the ring diagram technique is given by Patrón et al. (1997) and Basu, Antia & Tripathy (1999). Given the difficulty in determining the properties of high-degree modes from global mode analyses due to presence of leaks from adjoining  $\ell, m$  values (see e.g., Rhodes et al. 1998) and the fact that we are interested in studying the mode properties in localized regions, ring diagrams provide an alternative for such a study.

To extract the flow velocities and other mode parameters from the 3D power spectra we fit a model for peak profile to these spectra. The peak profiles are known to be asymmetric (Duvall et al. 1993; Nigam et al. 1998). Although the exact form of asymmetry is difficult to determine from the power spectra, the model suggested by Nigam & Kosovichev (1998) is found to fit the ring diagram spectra reasonably well (Basu & Antia 1999). Besides, use of asymmetric peak profile yields better agreement between frequencies determined by fitting the velocity and intensity spectra (Nigam et al. 1998; Basu, Antia & Bogart 2001). Thus we

adopt the model for asymmetric peak profile as used by Basu & Antia (1999) :

$$P(k_x, k_y, \nu) = \frac{\exp(A_0 + (k - k_0)A_1 + A_2(\frac{k_x}{k})^2 + A_3\frac{k_x k_y}{k^2})(S^2 + (1 + Sx)^2)}{x^2 + 1} + \frac{e^{B_1}}{k^3} + \frac{e^{B_2}}{k^4}, \quad (1)$$

where

$$x = \frac{\nu - ck^p - U_x k_x - U_y k_y}{w_0 + w_1(k - k_0)}, \quad (2)$$

$k^2 = k_x^2 + k_y^2$ ,  $k$  being the total wave number, and the 13 parameters  $A_0, A_1, A_2, A_3, c, p, U_x, U_y, w_0, w_1, S, B_1$  and  $B_2$  are determined by fitting the spectra using a maximum likelihood approach (Anderson, Duvall & Jefferies 1990). Here,  $k_0$  is the central value of  $k$  in the fitting interval and  $\exp(A_0)$  is the power in the ring, and we refer to this quantity as peak-height or power in the rest of the text. The coefficient  $A_1$  accounts for the variation in power with  $k$  in the fitting interval, while  $A_2$  and  $A_3$  terms account for the variation of power along the ring. The term  $ck^p$  is the mean frequency, while  $U_x k_x$  and  $U_y k_y$  represent the shift in frequency due to large scale flows. The fitted values of  $U_x$  and  $U_y$  give the average flow velocity over the region covered by the power spectrum and the depth range where the corresponding mode is trapped. The mean half-width is given by  $w_0$ , while  $w_1$  takes care of the variation in half-width with  $k$  in the fitting interval. The terms involving  $B_1, B_2$  define the background power, which is assumed to be of the same form as that of Patr3n et al. (1997). The asymmetry of the peak profiles is controlled by the parameter  $S$ . The form of asymmetric profile is the same as that prescribed by Nigam & Kosovichev (1998). The quantities  $U_x$  and  $U_y$  can be inverted to obtain the flow velocities in the east-west and north-south directions respectively (Basu, Antia & Tripathy 1999). The details of the fitting procedure are explained in Basu, Antia & Tripathy (1999) and Basu & Antia (1999). With asymmetric peak profile the calculated frequency ( $\nu = ck^p$ ) does not correspond to the point where power is maximum and the shift with respect to the point of maximum power will depend on the line width and the asymmetry parameter  $S$ . The extent of this shift can be calculated from the assumed peak profile.

In this work we use the data obtained by the Michelson Doppler Imager (MDI) on board the Solar and Heliospheric Observatory (SOHO) to determine the mode characteristics and the flow velocities in the outer part of the solar convection zone. We use the 3D spectra available in the MDI archives for this work. These spectra were obtained from an area covering  $128 \times 128$  pixels, i.e., about  $15^\circ \times 15^\circ$  in heliographic longitude and latitude, giving a resolution of  $0.03367 \text{ Mm}^{-1}$  or  $23.44 R_\odot^{-1}$ . The size of these regions is much larger than that of a typical sunspot, hence the average magnetic field over the region is smaller than the field inside the sunspots. Each region was tracked for 1664 minutes.

In order to estimate the influence of magnetic field we compare the mode characteristics in an active region with those in a quiet region at the same latitude and in the same Car-

rington rotation. There are a number of important reasons for this; the first being that the projection of the spherical solar surface onto a flat one introduces some fore-shortening that depends on the distance of the region from disk center, which can introduce systematic errors in determining the mode characteristics. To avoid this, we compare the results of an active region with that of a quiet region at the same latitude. Each region in a pair is therefore expected to have comparable effects of fore-shortening. In addition, to minimize the effects of fore-shortening, we have only used spectra obtained when the region under consideration was crossing the central meridian. Another reason for comparing pairs of active and quiet regions at the same latitude is that MDI images are known to have a certain amount of distortion which changes with latitude and longitude. By comparing regions at the same latitude and tracking them when they are at the central meridian we minimize errors due to this distortion.

The time constraint on the regions compared is imposed because the optical properties of the MDI instrument are known to change with time, resulting in changes in the scale converting pixel size to physical length. Since the scale length is needed to determine the mode properties in physical units, we need to ensure that we only compare mode properties of regions that have been analyzed within a small time interval.

For each of these regions we use a magnetic activity index (MAI) to denote the mean strong field. This quantity was calculated by integrating the unsigned field values within the same regions and over the same intervals as those over which the regions were tracked to calculate the power spectra, using available 96-minute magnetograms. The same temporal and spatial apodizations were used. Only the strong field index was calculated. This was done by setting all fields less than 50 Gauss to zero. One of the reasons of calculating just the strong field index, rather than the total field index is that the 96-minute magnetograms are a mix of 5-minute and 1-minute averages. The averages do have slightly different zero levels and noise levels, which can make a difference at low fields, but is not expected to make much difference if the quantity of interest is only the strong field index. In addition, to remove effects of cosmic rays, outliers were removed. These were defined as pixels with field values differing by a factor of more than six from the average of their neighbors, if that average was more than 400 G.

We have analyzed eighteen pairs of regions. These regions cover a reasonable range of latitudes within the active band and span a wide interval of time (from about March 1996 to June 2000). The coordinates of the regions studied, as well as the magnetic activity index of the regions, are tabulated in Table. 1. We determine the mode parameters for each region by fitting Eq. (1), and we compare the parameters for each pair. We believe that the difference in mode characteristics between an active and quiet region at the same latitude and during

the same Carrington rotation arises from the influence of magnetic fields. Some differences may also arise from temporal variations on short time-scales, but these are expected to be small. This can also be tested by comparing the characteristics in different quiet regions. In all cases we have found that differences in mode characteristics between two quiet regions is much less than the difference between a pair of active and quiet regions. Thus we believe that most of the difference between an active and quiet region characteristics is due to magnetic field.

### 3. Results

We have studied four main properties of the oscillation modes, viz., frequency, peak-height, line-width and the asymmetry parameter. We examine these one by one.

Frequencies of both f and p modes are higher in active regions than in quiet regions. This frequency shift is consistent with the expected effect of magnetic field (Campbell & Roberts 1989; Goldreich et al. 1991). Fig. 1 shows the relative frequency differences,  $\delta\nu/\nu = (\nu_{\text{active}} - \nu_{\text{quiet}})/\nu_{\text{quiet}}$ , between a few pairs of active and quiet regions. The mode frequencies are not only higher in active regions, but they also increase with the magnetic activity index (MAI) of the active region. The frequency differences increase with frequency and become as high as 1% for higher frequency modes, when the magnetic activity index is high. For clarity the error-bars are not shown in the figure, but the error is typically 0.0004 at frequencies around 3.5 mHz and increases to 0.0007 above 4.5 mHz. Furthermore, the relative frequency shift is overall an increasing function of frequency until about 5 mHz. We have not shown the results beyond this frequency as the fits to the modes are generally unreliable in these regions because of low power and large widths. These high frequency modes are not expected to be trapped inside the Sun.

Fig. 2 shows the frequency-averaged relative frequency differences between the active and quiet regions as a function of the MAI of the active region. The relative frequency differences are averaged over the frequency range of 2550 – 2750  $\mu\text{Hz}$  for f modes and 3000 – 3500  $\mu\text{Hz}$  for p modes. The averaging over the relatively narrow frequency range is necessary because of the frequency dependence of the frequency differences. The correlation coefficients between  $\delta\nu/\nu$  and the MAI are 0.89, 0.88, 0.92, and 0.89, for  $n = 0, 1, 2,$  and 3 modes respectively. We note that the frequency differences are almost linear with MAI, indicating that the strong field component of the magnetic field of the regions under study has a major effect on the frequency differences. The frequency shifts of f modes are comparable to those of p modes, which further suggests a direct magnetic influence on the oscillation modes, as any thermal perturbation would yield much lower shifts for f modes as compared to that for

p modes (e.g. Antia et al. 2001).

A striking feature of the frequency differences is that in all cases the frequency differences appear to be roughly independent of  $n$ . It may be noted that these frequency differences are not scaled by mode inertia, and hence the frequency variations cannot be explained as arising entirely from surface variations. A closer examination of Figs. 1 and 2 shows that the frequency shifts slowly increase with the radial order  $n$ , but this variation of  $\delta\nu/\nu$  with  $n$  cannot be accounted for by the corresponding variation in mode inertia. Thus the magnetic field must be penetrating below the outermost surface regions to produce the observed variation. In order to get more information about depth dependence of variation in Fig. 3 we show the same frequency differences plotted as a function of lower turning point of the modes. In this figure, the points for the different  $n$  stand apart, indicating that a major part of the frequency difference is a result of perturbations close to the surface. The modes for each  $n$  at high MAI appear to show sharp variations, but this feature occurs at different values of the lower turning point for modes of different radial order  $n$ . This feature is less conspicuous in Fig. 1 which shows the same frequency differences as a function of frequencies. We discuss this point and its implications in Section 4.

To show the variation in peak power we have plotted the ratio of the peak power in the active and quiet regions as a function of frequency in Fig. 4. The average error on each point is about 0.02 at about 3.5 mHz and increases to about 0.07 above 4.5 mHz. We notice that the f and p modes in active regions in general have lower power when compared with power in the quiet regions for the same modes. The peak power in the active region can be as low as a third of that in the quiet region for some modes. The suppression increases with increase in the MAI. Our results agree with early observations which showed that power is reduced in active regions (Tarbell et al. 1988; Hindman & Brown 1998).

The change in peak power is not monotonic with frequency. Maximum suppression seems to occur in the frequency range of about 3 mHz to 3.5 mHz. This is similar to results of Bogdan et al. (1993) who found maximum absorption around wavenumber  $k \approx 0.8 \text{ Mm}^{-1}$  or  $\ell \approx 550$ . This value of  $\ell$  approximately agrees with the values where we find maximum suppression of power for  $n = 1, 2$  modes. It is not clear if the mode absorption can be compared with suppression of power in the sunspot region, since the absorption is measured for traveling waves, while the modes we are studying are standing wave pattern. The suppression of power decreases as the radial order  $n$  of the modes increases. There is a gradual shift of the position of maximum suppression towards higher frequencies with increase in  $n$ . At high frequencies, the suppression tends to become small and at low MAI it may change sign and become a power enhancement instead. Similar behavior has been found by Hindman & Brown (1998).

Fig. 5 shows the relative difference in half-width  $w_0$  of the modes, between the active and quiet regions, plotted as a function of frequency. On average the error on each point is about 0.02 at 3.5 mHz and increases to about 0.04 above 4.5 mHz. The half-width of a peak profile in the power spectrum is related to the imaginary part of the frequency and hence is an indication of mode-damping. The life-time of a mode is inversely proportional to its half-width. The half-widths  $w_0$  of the f and p modes in the active regions are generally larger than those in the quiet regions, at least for  $\nu > 2.5$  mHz. Thus it appears that most modes live longer in quiet regions than they do in active regions, implying additional damping in active regions. The change is generally larger for high magnetic field regions. The maximum change in the width occurs in the frequency range 3 mHz to 3.5 mHz, quite similar to the behavior of maximum power suppression. The change in the width seems to decrease with increasing mode order, the f modes showing the largest change. A similar variation in line-widths of global p modes has been found with solar cycle (Komm, Howe & Hill 2000). The variation in global mode widths is much less ( $\approx 3\%$ ) than what we find, presumably because of smaller variations in the average global magnetic field. Based on their observations for global modes, Komm, Howe & Hill (2000) predict an increase by up to 38% in widths and a reduction of up to 70% in mode area in active regions (the change in mode areas is shown in Fig. 6 and discussed below). It is not clear what field strength they have assumed for the active regions, but our results at high MAI are comparable to their predictions. For example, for the highest MAI of 104.4 G in our sample, we find a maximum increase by about 50% in widths (Fig. 5) and a maximum reduction of about 55% in mode area (Fig. 6), for  $n=1$  mode. The situation is not completely clear for lower frequency modes. In any case it is difficult to determine the width of low frequency modes reliably using ring diagram analysis, since the actual width is smaller than the resolution of the power spectra.

Given that the total power in the mode is the area under the peak in the power spectrum, it is not instantly clear whether the increase in the line widths in active regions compensates for the decrease in the peak height. The area under a peak is a measure of excitation for the corresponding mode. To check for this variation we have plotted the ratio of the product of peak height and half-widths  $A_0 w_0$  as a proxy for the area under the peak. The area should be a measure of acoustic power of the mode and hence should contain information about mode excitation. This quantity is plotted in Fig. 6. The figures show that power in the modes is indeed lower in high-activity regions. This is true even at low frequencies. However, there seems to be some enhancement of power at higher frequencies ( $> 4$  mHz), particularly at low and intermediate magnetic activity index.

The detection of the oscillation modes crucially depends on the signal-to-noise ratio; hence it is important to compare the background noise in the power-spectra, between the active and quiet regions. The background in solar power-spectra is not completely noise,



but has a large component of so-called “solar noise”, which is the background produced by convective cells. The expression for the background in Eq. 1 has two terms with different  $\ell$  dependences. We add the two terms after taking the different  $\ell$  dependence into account (i.e., we calculate  $\exp(B_1)\ell + \exp(B_2)$ ). The background is predominantly a function of the degree  $\ell$  of the mode, rather than the frequency. We have plotted the ratio of background in the active and quiet regions as a function of degree in Fig. 7. The average error on each point is about 0.07. For most modes the background in active region is less than that in quiet region. It may be noted that background should really be a function of  $\nu$  and  $\ell$ , but since we have determined it only in neighborhood of a peak we have labeled the points by the corresponding value of  $n$ . At high frequencies it is difficult to determine the background reliably, as the peak widths are large. Hence the tails of the Lorentzian profiles extend quite far and thus the ‘background’ between two peaks is mostly contributed by the tails of the peak profiles. That is why we have not shown the background at high frequencies or high  $n$ . No significant variation in background power with solar cycle has been found by Komm, Howe & Hill (2000) in their analysis using global modes. The expected variation in the background due to small increase in average magnetic field with solar cycle may be too small. Global mode analysis is also restricted to  $\ell < 200$ , where the variation is small even in our results.

We can see from Fig. 7 that the background in the active regions is generally lower than that in the quiet regions. The reduction may be expected because magnetic field is known to suppress convection, which is the main source of background in power spectra. There is a steep dependence of the background on the degree of the mode at intermediate values of MAI; the situation at high MAI is not very clear. At intermediate MAI, there appears to be a minimum in the background ratio around  $\ell = 1000$ , which corresponds to a horizontal wavelength of about 4 Mm. This length scale is somewhat larger than the granulation length scale, but much smaller than the mesogranulation scale.

The asymmetry parameters for  $n = 0$  and  $n = 1$  modes for different regions are plotted in Fig. 8. The average error on each point is about 0.005 at 3.5 mHz. The  $n = 2$  modes have not been plotted for the sake of clarity; their behavior is very similar to that of the  $n = 1$  modes. An asymmetry parameter of  $S = 0$  implies symmetric peaks. A negative asymmetry implies that power in the low frequency half of the peak is higher than that in the high frequency part. The larger the absolute value of the asymmetry parameter, the more asymmetric is the peak. We see that the asymmetry of the modes increases with increase in the magnetic activity index of the region under consideration. This is true for all the modes. The asymmetry of the line profile is generally an indication of the depth at which the modes are excited (Kumar & Basu 1999). The deeper a mode is excited, the more symmetric is the peak. The increase in the asymmetry of the profile can therefore be an indication of the

fact that the modes in the active regions are excited closer to the surface of the Sun than the modes in the quiet regions.

As we did for the frequency shifts (Fig. 2), we also study the variation of the other mode parameters against the MAI of all the active regions selected. The results are shown in Fig. 9. The frequency-averaged relative width differences are plotted in Fig. 9a. Although the results show a somewhat large scatter, it is pretty clear that the line-widths increase with the increase of MAI. The correlation coefficients between the relative variation in width and the MAI turn out to be 0.49, 0.86, and 0.69 for  $n = 0, 1, 2$  respectively. The correlation is not strong, which is reflected in the scatter. The scatter could indicate that the widths are affected by the overall magnetic field and not merely the strong-field component.

The frequency-averaged peak power ratios, as a function of the MAI, are plotted in Fig. 9b. We note the general trend of increasing power suppression with MAI, however, there seems to be a saturation effect at high activity index. The correlation coefficients between the power ratio and MAI are  $-0.56, -0.75, -0.58$  for  $n = 0, 1, 2$  respectively. Thus it is clear that variation in power is only weakly correlated with MAI, probably because of saturation at high field.

Fig. 9c shows how the frequency-averaged asymmetry parameter varies as a function of the MAI. The increase in asymmetry seems to be monotonic with MAI, though with some scatter. We note that Goode & Strous (1996) (see also, Rimmele et al. (1995)) have observed so called “seismic events”, which occur in the dark intergranular lanes and are shown to excite the solar oscillations. They have shown that a local magnetic field suppresses both the acoustic flux and the p-mode power. These observations are of a quiet region, showing that even a weak magnetic field significantly suppresses the acoustic energy flux due to seismic events. Hence, our result that the mode asymmetry parameter increases with the magnetic field in active regions implying excitation of the modes closer to the surface might seem contradictory to the results of Goode & Strous (1996) at first sight. But it should be noted that the power in modes is reduced in the active regions, thus demonstrating that excitation is reduced. This reduction in excitation probably shifts the effective source of excitation upwards, as the reduction itself will also have some depth dependence. It may also be possible that the magnetic field induced activity at and above the surface layers, like the flaring activities, may play a role in the excitation of oscillation modes in active regions (Kosovichev & Zharkova 1998), thus pushing the effective excitation sources upwards.

The dependence of the degree-averaged background ratio on the MAI is shown in Fig. 9d. We note that the ratio seems to decrease with MAI though there is a large scatter. The f-mode background however, decrease reasonably monotonically with MAI. The correlation coefficient between the background ratio and MAI is  $-0.52$  for  $n = 0$  and  $-0.40$  for  $n = 1$ .

Thus it can be seen that the correlation between background and MAI is rather weak as is apparent from the large scatter in the Fig. 9d.

Although flow velocity of solar plasma is not a mode characteristic, we can determine the zonal and meridional flow components from the ring diagram analysis. Unlike in the case of the other parameters, we are unable to discern any systematic change in the flow velocities with magnetic field and hence the results are not shown. The flow velocities are different in the quiet and active zones, but we cannot find a systematic pattern in the changes with magnetic field. Since we are effectively looking at averages over a region much larger than the size of active region, the flows may also be averaged giving more complex behavior. Haber et al. (2001) have made more detailed study of flows in active region using ring diagram analysis and they claim a general increase in the flow velocities in active regions. Our sample of regions studied is too limited to make detailed comments.

#### 4. Discussion and Conclusions

In this work we have performed plane-wave analyses of different active regions of the Sun to study how mode characteristics of solar oscillations change in these regions as compared with quiet regions at the same latitude. We find that the characteristics of both f and p modes in the active regions are different from those in quiet regions. The change, in most cases, varies with the MAI which is a measure of the average strong magnetic field of the region under study.

As with the solar cycle related variation of low and intermediate degree modes (Libbrecht & Woodard 1990), the frequencies of high-degree modes increase with increase in the mean magnetic field of the area under study. The frequency shifts of f and p modes are comparable. This suggests that the main cause of the frequency shifts is the magnetic field and not any kind of change in solar structure. Changes in structure shift f mode frequencies by much smaller amounts than they do p-mode frequencies. Furthermore, it appears that the frequency shifts for modes of different degrees cannot be explained as being due to differences in the mode inertia of these modes. This gives us a handle on the penetration depth of the magnetic fields. From Fig. 3 it can be seen that the lower turning point of all modes considered in this study is below a depth of 1.5 Mm from the solar surface. The magnetic fields must therefore penetrate below this depth to explain the observed frequency variation, which can not then be a purely surface effect. Considering that the relative frequency differences are of the order of  $10^{-2}$ , the ratio of magnetic to gas pressure in active regions should be of this order to explain the observed frequency shifts. This gives a magnetic field of about 100 G near the solar surface and correspondingly larger values in the interior. The

surface field is consistent with the actual mean value inferred from the magnetograms in the region that we have considered.

It is, however, difficult to find a magnetic field configuration which will yield observed frequency shifts characterized by a variation which depend mostly on frequency alone without scaling by mode inertia. Wilson depression in sunspots is another possible mechanism to explain the frequency shifts and power reduction (Hindman et al. 2001). Since the effective depression can be expected to reduce with increasing depth, it may explain the increase in frequency shift with frequency because the higher frequency modes are reflected in higher layers. The depression can also explain the comparable shifts in f- and p-mode frequencies since the layers in which these modes are effectively trapped will also be depressed. From Fig. 1 it can be seen that at highest field considered the relative shift in f-mode frequency could be 0.005, which will require depression by about 2Mm. Depression by such a magnitude is probably not expected. Thus it is quite possible that actual frequency shift is due to a combination of direct effects of magnetic fields and of structural variations like the Wilson depression. Any model to explain the frequency shift should also be required to obtain f-mode shifts by amount comparable to those for p modes.

The relative frequency shifts in active regions are found to have an overall increase with frequency up to a frequency of about 5 mHz. For modes of intermediate degree, Libbrecht & Woodard (1990), using data obtained at Big Bear Solar Observatory (BBSO), found frequency shifts which have a maximum around 4 mHz and then tend to reduce. It is difficult to fit individual modes in this frequency range due to large widths and it becomes necessary to use ridge fitting techniques to study these modes. The ridge fitting techniques have larger uncertainties and it is not clear if the decrease in frequency shift seen in BBSO data is real. Ring diagram analysis is also essentially a ridge fitting technique but the spectra are not expected to be affected by leaks arising from neighboring  $\ell, m$  values. We do not find any decrease in frequency shift with frequency. Similar results have been found by Hindman et al. (2001) also using ring diagram analysis. Their results are consistent with ours.

The peak power of the modes in active regions is considerably smaller than that in the quiet regions. This reduction in peak power seems to have contributions from both acoustic absorption and reduced excitation in active regions. Other possible mechanisms for the reduction of power in active regions are the modification of the p-mode eigenfunctions in magnetic region (Hindman et al. 1997) or the fact that the height of formation of the spectral lines used to study oscillations is affected by magnetic field. A discussion of various mechanisms for the absorption of p-mode power can be found in Spruit (1996).

It is clear that there is a power enhancement in the high frequency modes at low and intermediate field strengths, while the exact values of field strength at which the transition

to power reduction occurs seem to depend on the radial order  $n$  and it is not clear, though it is seen that higher  $n$  modes show larger power enhancement. We note that such ‘halos’ of high- $\nu$  power enhancements for low and intermediate field strengths have been reported in the literature (Hindman & Brown 1998; Thomas & Stanchfield 2000) mainly at frequencies above the acoustic cut-off (5.0 mHz). This feature has been suggested to be due to some mode of oscillation that is not purely acoustic in nature, by Thomas & Stanchfield (2000), possibly due to magnetic modes of oscillations in plage flux tubes that surround strongest field spot regions (Hindman & Brown 1998). It has also been reported by Lindsey & Braun (1999) using a different technique that sunspots are surrounded by acoustic “halos” of excess power at frequencies above 5 mHz, which they attribute to a large scale eddy circulation induced by the convective energy blocked by the sunspots.

The lower background power in the active regions seems to reinforce the idea that high magnetic fields could hinder convection (Biermann 1941; Chandrasekhar 1961) which is the source of solar noise. The asymmetry in peak profile is believed to be an indicator of depth of source of excitation, and an increase in asymmetry with magnetic field implies a decrease in depth of source. The decrease in the excitation depth with the increase in magnetic field implies that the turbulence which excites the modes is pushed upwards towards the surface. Goode & Strous (1996) find suppression of acoustic flux and p-mode power even in a weak magnetic field quiet region. We believe that magnetic field induced activities in the surface and higher layers may play a role in the excitation of oscillation modes in the active regions. Indeed, solar flares have been observed (Kosovichev & Zharkova 1998) to excite seismic activity in the active regions. The width of peak profiles also increase with magnetic field, implying a shorter lifetime and hence higher damping due to magnetic field. This is consistent with the results of Bogdan et al. (1996).

In conclusion we find that mode parameters change as a result of magnetic fields in active regions. Judging by the frequency shifts, the influence of the magnetic fields seems to penetrate to at least 1.5 Mm. Unfortunately, these data are not yet precise enough to determine the magnetic field by inversion. The power in the modes is smaller in active regions than in quiet regions, while the modes are more asymmetric indicating a shallower excitation depth.

We would like to thank Richard S. Bogart for providing the magnetic activity indices. This work utilizes data from the Solar Oscillations Investigation/ Michelson Doppler Imager (SOI/MDI) on the Solar and Heliospheric Observatory (SOHO). The MDI project is supported by NASA grant NAG5-8878 to Stanford University. SOHO is a project of international cooperation between ESA and NASA. This work was supported in part by NASA Grant # NAG5-10912 to SB.

## REFERENCES

- Anderson, E. R., Duvall, T. L., Jr., & Jefferies, S. M. 1990, *ApJ*, 364, 699
- Antia, H. M., Basu, S., Pintar, J., Schou, J. 2001, submitted
- Basu, S., & Antia, H. M. 1999, *ApJ*, 525, 517
- Basu, S., & Antia, H. M. 2000, *Sol. Phys.*, 192, 469
- Basu, S., Antia, H. M., & Tripathy, S. C. 1999, *ApJ*, 512, 458
- Basu, S., Antia, H. M., & Bogart, R. S. 2001, in *Proc. SOHO 10/GONG 2000 Workshop on Helio- and Asteroseismology at the Dawn of the Millennium*, ESA SP-464, Ed. A. Wilson, p. 183.
- Bhatnagar, A., Jain, K., & Tripathy, S. C. 1999, *ApJ*, 521, 885
- Biermann, L. 1941, *Vierteljahrsschr. Astron. Ges.*, 76, 194
- Bogdan, T. J., Brown, T. M., Lites, B. W., Thomas, J. H. 1993, *ApJ*, 406, 723
- Bogdan, T. J., Hindman, B. W., Cally, P. S., Charbonneau, P. 1996, *ApJ*, 465, 406
- Braun, D. C. 1995, *ApJ*, 451, 859
- Braun, D. C., La Bonte, B. J., & Duvall, T. L., Jr. 1987, *ApJ*, 319, L27
- Braun, D. C., La Bonte, B. J., & Duvall, T. L., Jr. 1988, *ApJ*, 335, 1015
- Braun, D. C., La Bonte, B. J., & Duvall, T. L., Jr. 1990, *ApJ*, 354, 372
- Braun, D.C., & Lindsey, C. 1999, *ApJ*, 513, L79
- Campbell, W.R., & Roberts, B. 1989, *ApJ*, 338, 538
- Chandrasekhar, S. 1961, *Hydrodynamic and Hydromagnetic Stability* (Oxford: Clarendon)
- Duvall, T. L., Jr., Jefferies, S. M., Harvey, J. W., Osaki, Y., & Pomerantz, M. A. 1993, *ApJ*, 410, 829
- Dziembowski, W. A., Goode, P. R., di Mauro, M. P., Kosovichev, A. G., & Schou, J. 1998, *ApJ*, 509, 456
- Elsworth, Y., Howe, R., Isaak, G. R., McLeod, C. P., & New, R. 1990, *Nature*, 345, 322

- Goldreich, P., Murray, N., Willette, G., & Kumar, P. 1991, *ApJ*, 370, 752
- Goode, P. R., & Strous, L. H. 1996, *Bull. Astr. Soc. India*, 24, 223
- Haber, D. A., Hindman, B. W., Toomre, J., Bogart, R. S., & Hill, F. 2001, in *Proc. SOHO 10/GONG 2000 Workshop on Helio- and Asteroseismology at the Dawn of the Millennium*, ESA SP-464, Ed. A. Wilson, p213
- Hill, F. 1988, *ApJ*, 333, 996
- Hindman, B. W., & Brown, T. M. 1998, *ApJ*, 504, 1029
- Hindman, B. W., Haber, D. A., Toomre, J., & Bogart, R. S. 2001, in *Proc. SOHO 10/GONG 2000 Workshop on Helio- and Asteroseismology at the Dawn of the Millennium*, ESA SP-464, Ed. A. Wilson, p143
- Hindman, B. W., Jain, R., & Zweibel, E. G. 1997, *ApJ*, 476, 392
- Hollweg, J. V. 1988, *ApJ*, 335, 1005
- Howe, R., Komm, R., & Hill, F. 1999, *ApJ*, 524, 1084
- Keppens, R., Bogdan, T. J., & Goossens, M. 1994, *ApJ*, 436, 372
- Komm, R. W., Howe, R., & Hill, F. 2000, *ApJ*, 531, 1094
- Kosovichev, A. G., & Zharkova, V. V. 1998, in *IAU Symposium 185 New Eyes to See Inside the Sun and Stars*, eds. F. L. Deubner, J. Christensen-Dalsgaard, & D. Kurtz, p183
- Kumar, P., & Basu, S. 1999, *ApJ*, 519, 396
- Libbrecht, K. G., & Woodard, M.F. 1990, *Nature*, 345, 779
- Lindsey, C., & Braun, D. C. 1999, *ApJ*, 510, 494
- Nigam, R., Kosovichev, A. G. 1998, *ApJ*, 505, L51
- Nigam, R., Kosovichev, A. G., Scherrer, P. H., & Schou, J. 1998, *ApJ*, 495, L115
- Patrón, J., et al. 1997, *ApJ*, 485, 869
- Patrón, J., González Hernández, I., Chou, D.-Y., & The TON Team 1998, *ApJ*, 506, 450
- Rhodes, E. J., Jr., Reiter, J., Kosovichev, A. G., Schou, J., & Scherrer, P. H. 1998, in *SOHO-6/GONG 98 Workshop Abstract*, p-73

Rimmele, T. R., Goode, P. R., Harold, E., & Stebbins, R. T. 1995, *ApJ*, 444, L119

Rosenthal, C. S 1990, *Sol. Phys.*, 130, 313

Spruit, H. C. 1996, *BASI*, 24, 211

Tarbell, T. D., Peri, M., Frank, Z., Shine, R., & Title, A. M. 1988, in *Seismology of the Sun and Sun-Like Stars*, ed. E. Rolfe (ESA SP-286), p 315

Thomas, J. H., & Donald C. H. Stanchfield II 2000, *ApJ*, 537, 1086



Table 1: Co-ordinates and Magnetic Activity Index of Regions Analyzed

CR *	Latitude (deg.)	CR Longitude (active) (deg.)	Magnetic Index (active) (Gauss)	CR Longitude (quiet) (deg.)	Magnetic Index (quiet) (Gauss)
1933	22.5S	30	91.19	180	0.28
1934	22.5N	285	26.77	165	0.38
1934	22.5S	225	48.53	315	0.99
1934	22.5S	90	39.38	165	0.44
1947	22.5N	270	59.94	30	3.61
1947	30.0S	255	28.21	45	1.85
1948	22.5N	285	71.00	330	2.71
1948	15.0S	105	40.94	60	1.14
1948	22.5N	30	57.15	120	3.09
1949	22.5N	300	54.97	120	1.50
1949	22.5S	225	43.44	60	1.10
1949	22.5N	210	58.62	60	5.22
1949	15.0S	120	38.09	60	0.80
1949	30.0N	90	15.91	120	2.11
1963	15.0S	180	59.88	105	1.89
1963	22.5N	75	104.45	225	1.80
1964	22.5N	285	80.52	105	...
1964	15.0S	120	61.37	90	2.98

---

\*Carrington Rotation

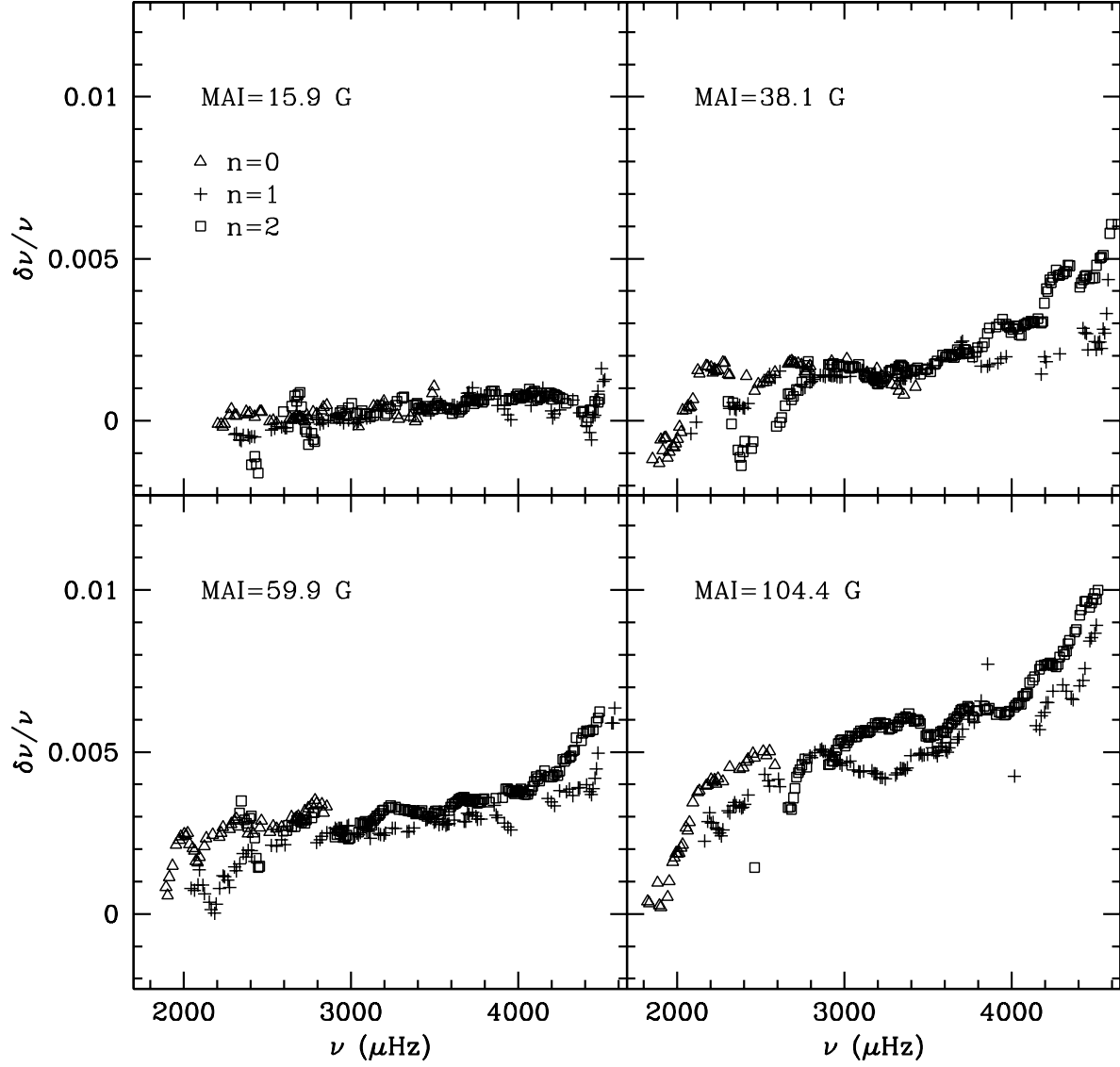


Fig. 1.— The relative frequency differences as a function of frequency for four different pairs of regions. The error on the points is about 0.0004 at 3.5 mHz and increases to 0.0007 above 4.5 mHz. The MAI for the active region in each pair is indicated in the panels.

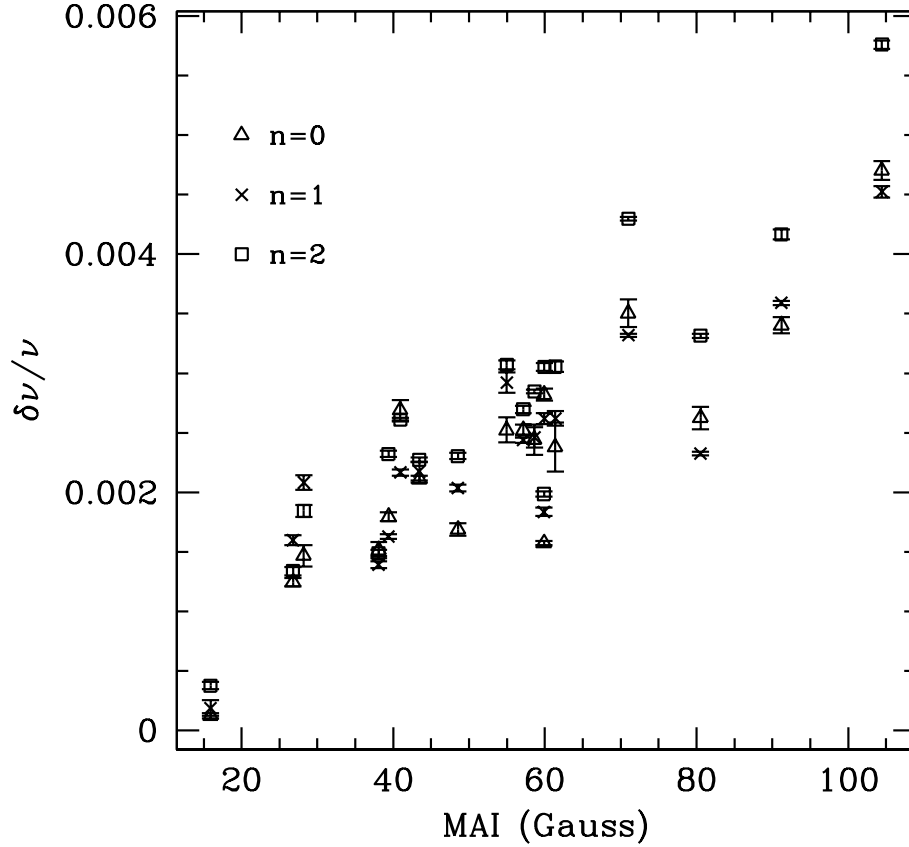


Fig. 2.— The average relative frequency differences plotted as a function of the magnetic activity index. Frequency differences of f modes have been averaged over modes in the frequency range 2550 to 2750  $\mu\text{Hz}$ , while those of p modes have been averaged over modes in the range 3000 to 3500  $\mu\text{Hz}$ . The averaging over the relatively narrow frequency range is necessary because of the steep frequency dependence of  $\delta\nu/\nu$ .

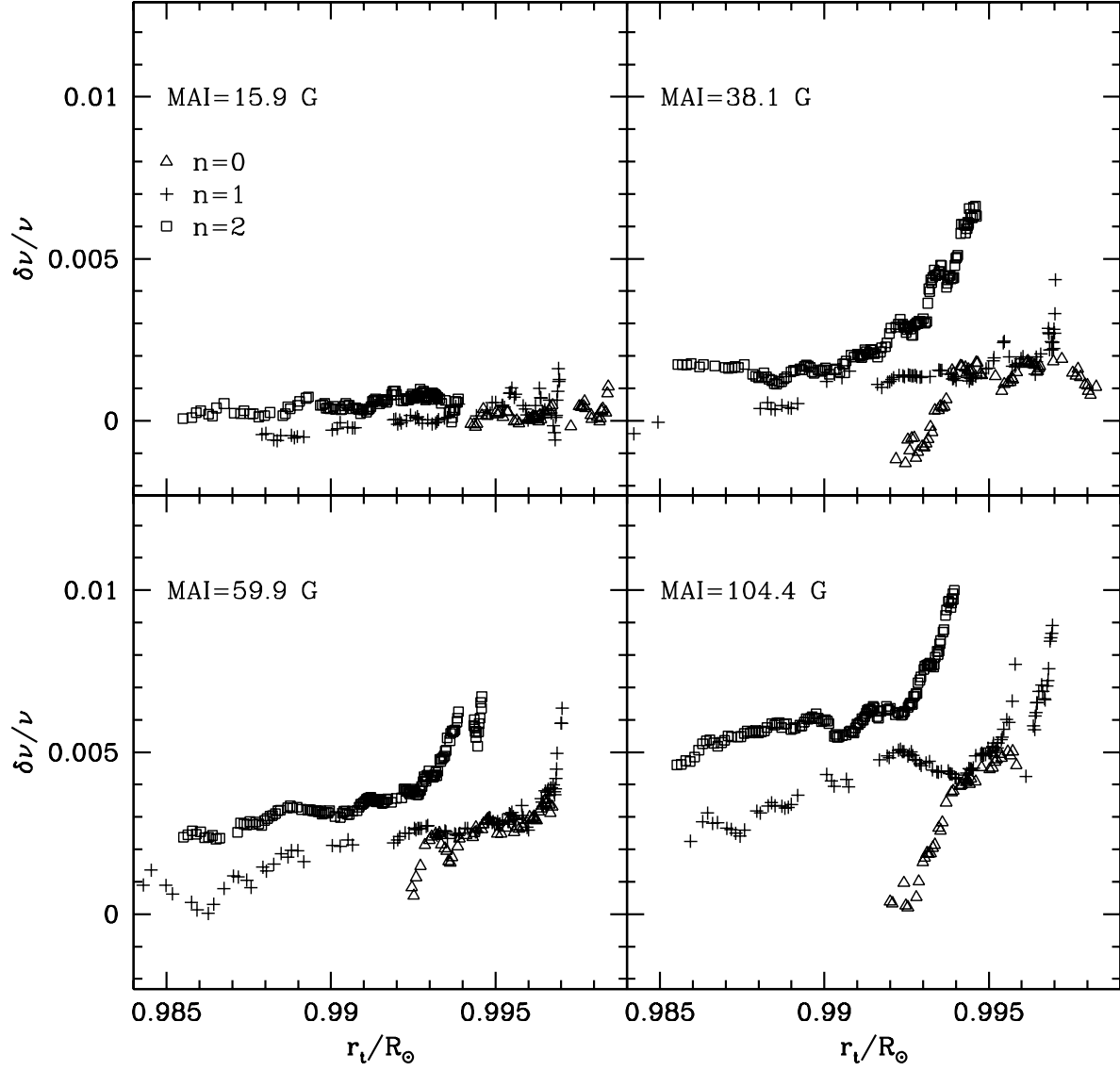


Fig. 3.— The relative frequency differences as a function of lower turning point of the modes, for four different pairs of regions. The MAI for the active region in each pair is indicated in the panels.

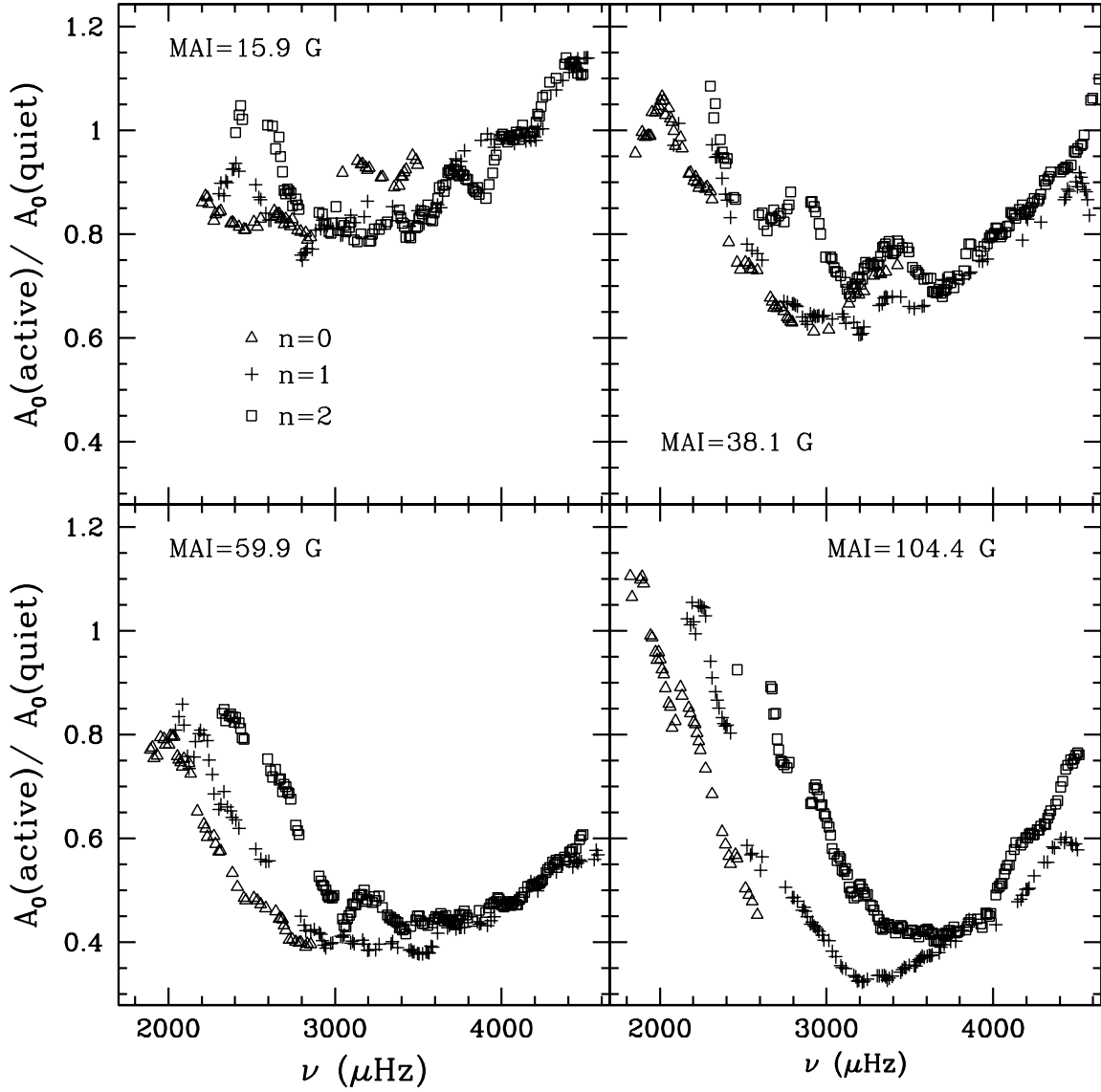


Fig. 4.— The ratio of the peak power between pairs of active and quiet regions. The error on the points is about 0.02 at 3.5 mHz and increases to 0.07 at 4.5 mHz. The MAI of the active regions is indicated in the panels.

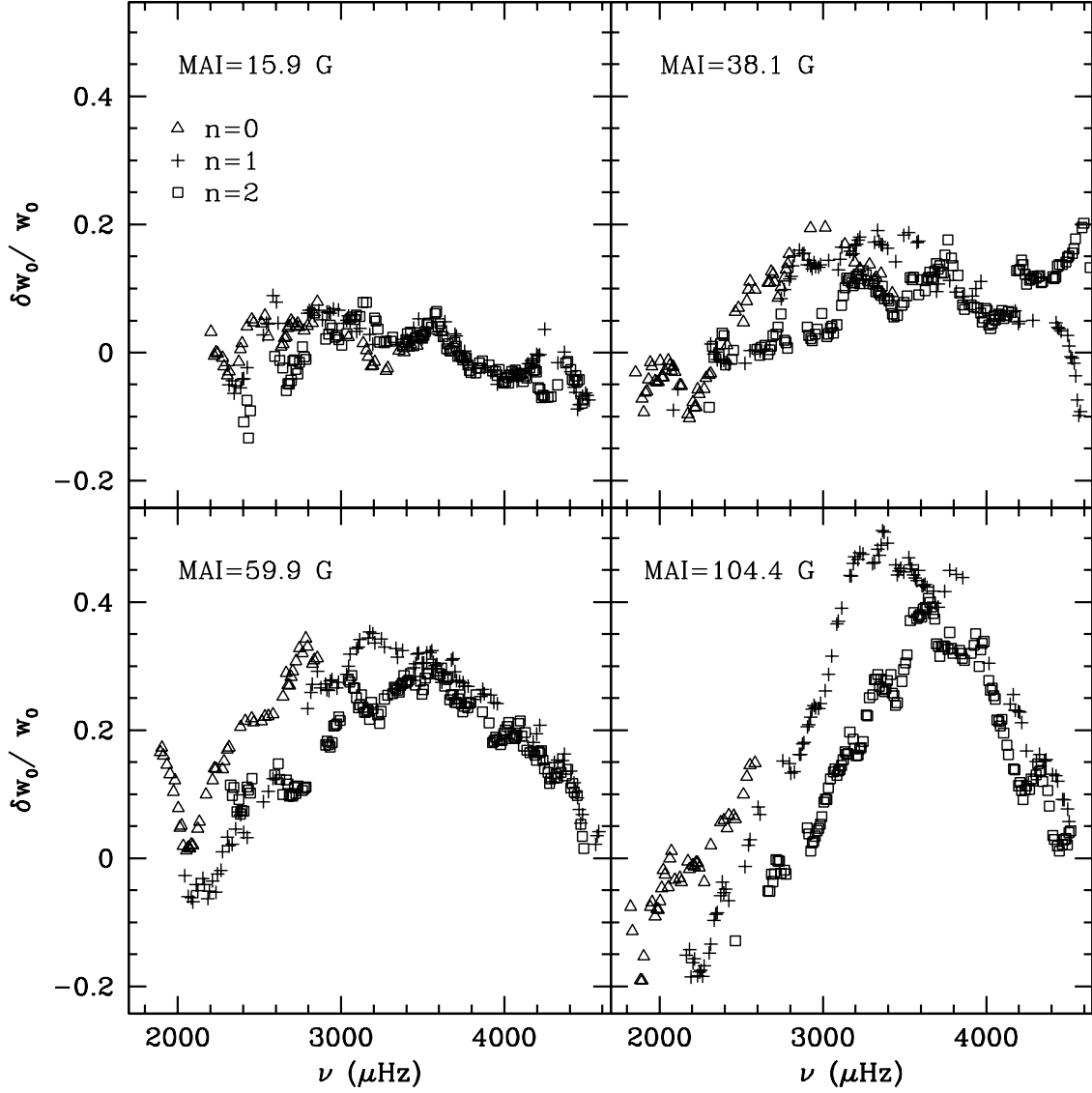


Fig. 5.— The fractional differences in the mode line widths,  $\delta w_0 / w_0 = (w_{0,\text{active}} - w_{0,\text{quiet}}) / w_{0,\text{quiet}}$ , as a function of frequency for four different pairs of regions. The errors on the points increase from being about 0.02 at 3.5 mHz to 0.04 above 4.5 mHz. The MAI for the active region in each pair is indicated in the panels.

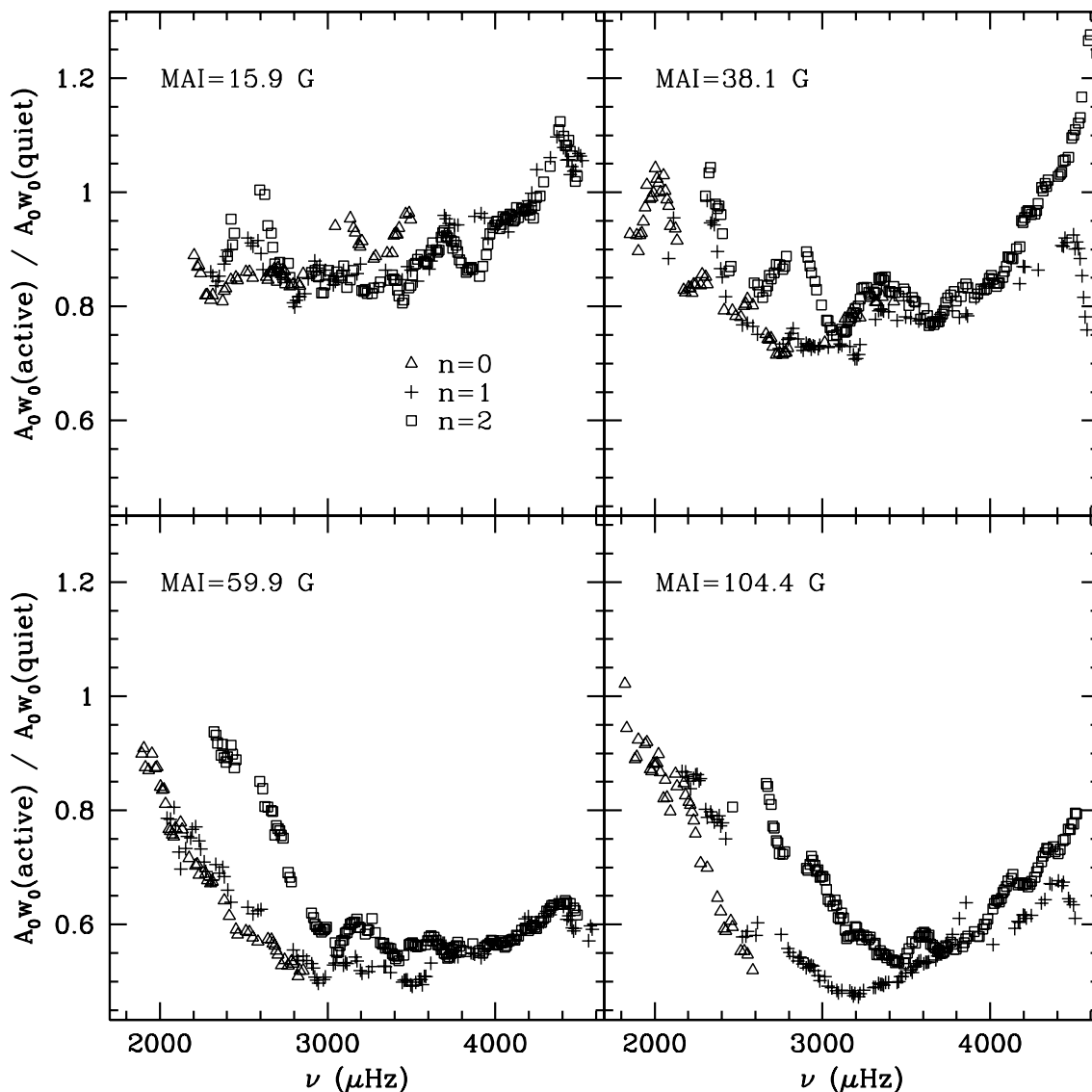


Fig. 6.— The ratio of the product of the peak height and half-width of the modes plotted as a function of frequency for four different pairs of regions. The MAI for the active region in each pair is indicated in the panels.

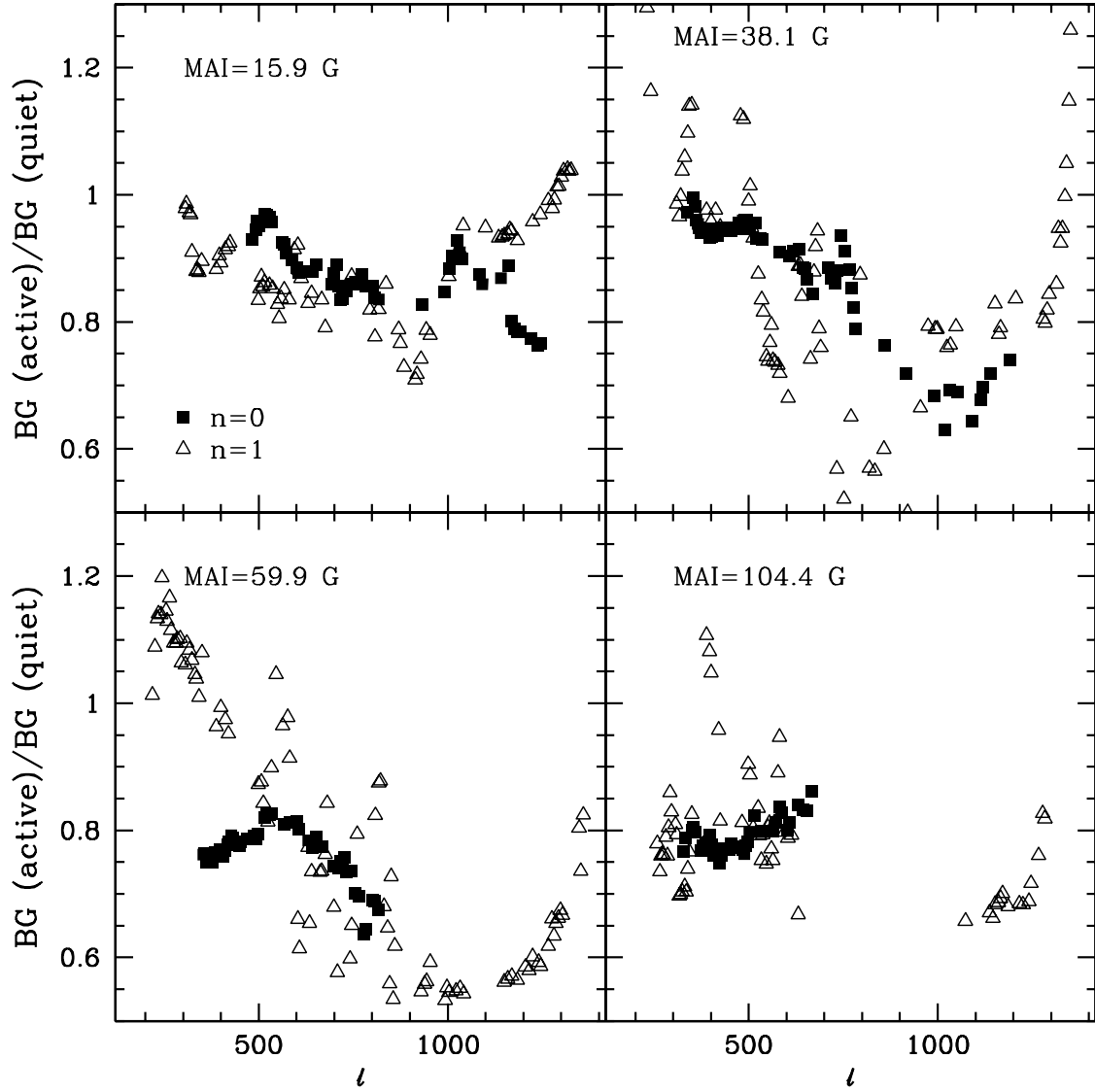


Fig. 7.— The ratio of the background noise in the active and quiet regions plotted as a function of degree for four different pairs of regions. The errors on the points are about 0.07. The MAI for the active region in each pair is indicated in the panels.



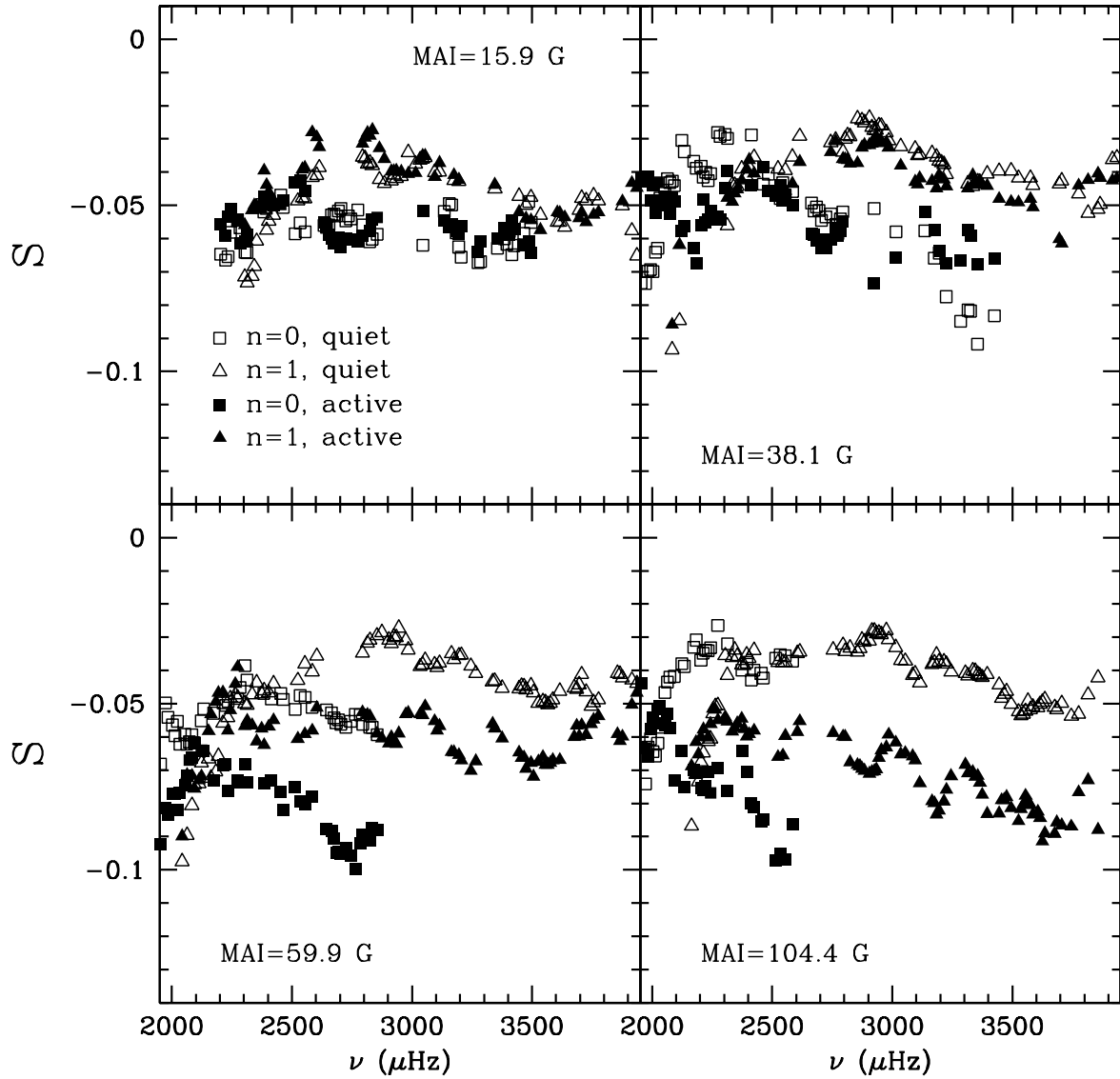


Fig. 8.— The mode asymmetry parameter,  $S$ , as a function of frequency for four different pairs of active and quiet regions. The average error on each point is about 0.005. The MAI of the active regions is indicated in the panels.

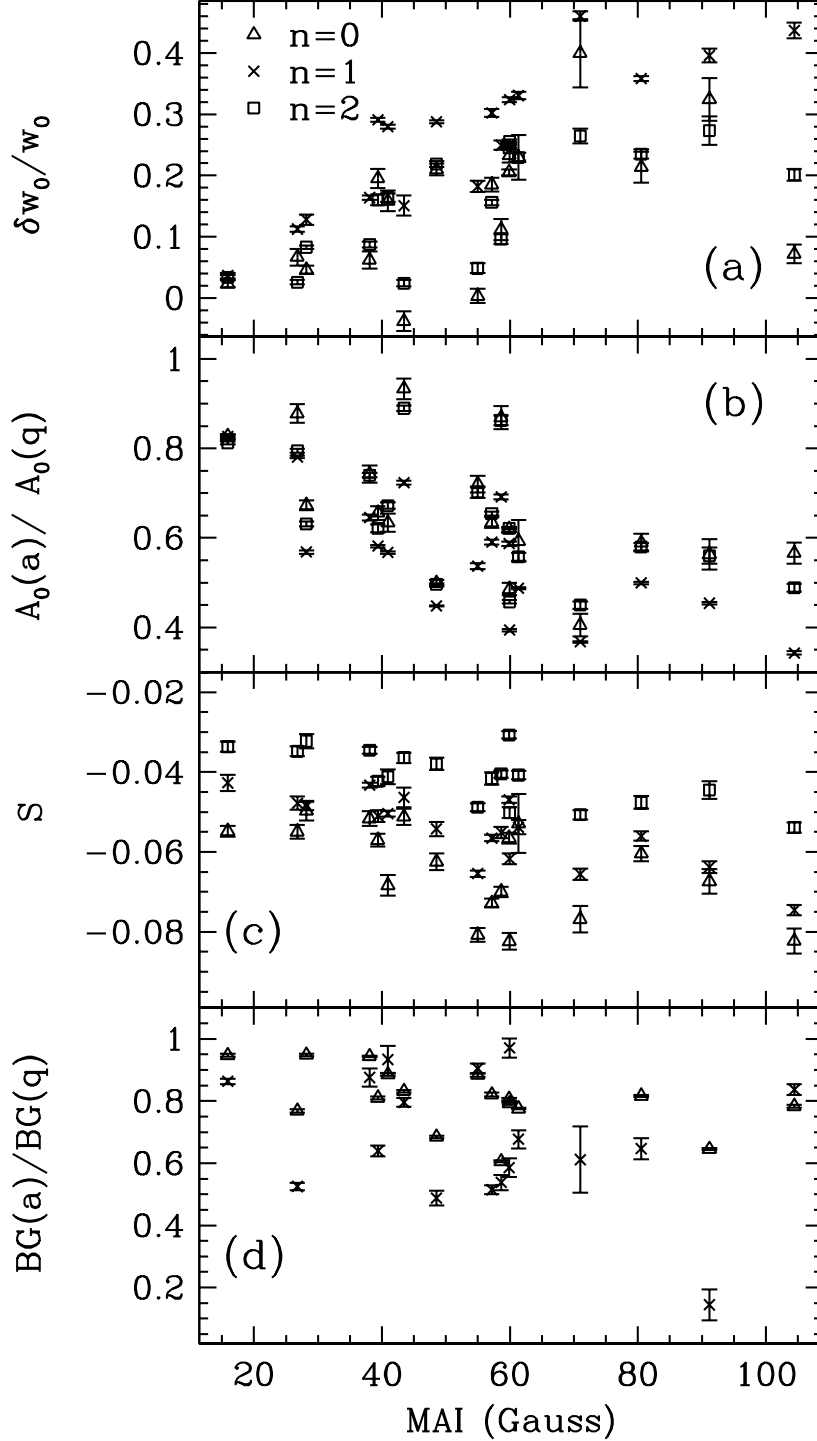


Fig. 9.— The frequency-averaged mode parameters against the MAI of the active regions; *a*) fractional differences in the mode line widths, *b*) peak power ratios, *c*) the asymmetry parameter  $S$  and *d*) the ratio of the background noise in the active and quiet regions averaged over the mode degree range  $\ell = 400$  to  $\ell = 600$ . The labels “a” and “q” in the axis labels imply active and quiet regions respectively.